

Exosomal Long Noncoding RNA HOXD-AS1 Promotes Prostate Cancer Metastasis via miR-361-5p/FOXM1 Axis

Yongming Jiang

Kunming Medical University First Affiliated Hospital

Hui Zhao

Kunming Medical University First Affiliated Hospital

Yuxiao Chen

Kunming Medical University First Affiliated Hospital

Kangjian Li

kunming yike daxue fushu qujing yiyuan: Kunming Medical University Affiliated Qujing Hospital

Jianheng Chen

Kunming Medical University First Affiliated Hospital

Tianjie Li

Kunming Medical University First Affiliated Hospital

Baiyu Zhang

Kunming Medical University First Affiliated Hospital

Caifen Guo

Kunming Medical University First Affiliated Hospital

Liangliang Qing

Kunming Medical University First Affiliated Hospital

Jihong Shen

Kunming Medical University First Affiliated Hospital

Xiaodong Liu

Kunming Medical University First Affiliated Hospital

Peng Gu (✉ gupeng@ydy.cn)

Kunming Medical University First Affiliated Hospital <https://orcid.org/0000-0002-9646-172X>

Research

Keywords: Prostate Cancer (PCa), Metastasis, Exosome, Long noncoding RNA (lncRNA), miR-361-5p

Posted Date: July 30th, 2021

DOI: <https://doi.org/10.21203/rs.3.rs-736613/v1>

License:  This work is licensed under a Creative Commons Attribution 4.0 International License.

[Read Full License](#)

Version of Record: A version of this preprint was published at Cell Death & Disease on December 1st, 2021. See the published version at <https://doi.org/10.1038/s41419-021-04421-0>.

Abstract

Background: Development of distant metastasis is the main cause of deaths in prostate cancer (PCa) patients. Understanding the mechanism of PCa metastasis is of utmost importance to improve its prognosis. The role of exosomal long noncoding RNA (lncRNA) has been reported yet fully understood in the metastasis of PCa.

Methods: Co-culture assay, in-situ hybridization and quantitative PCR (qPCR) were applied to identify the presence of HOXD-AS1 overexpressing exosomes secreted by of castration resistant prostate cancer (CRPC) cells. Migration and wound healing assays were carried out to evaluate the biological function of exosomal HOXD-AS1. Then a mouse model was used to elucidate the effect of exosomal HOXD-AS1 on distant metastasis of PCa *in vivo*. Further RNA immunoprecipitation and luciferase assay were applied to identify the interaction between HOXD-AS1 and miR-361-5p. Moreover, rescue experiment was conducted to prove the binding of exosomal HOXD-AS1 and miR-361-5p. Last but not least, the application of serum exosomal HOXD-AS1 as a diagnostic and prognostic biomarker for PCa was evaluated.

Results: We discovered the exosomal lncRNA HOXD-AS1 is upregulated in CRPC cell line derived exosomes and serum exosomes from metastatic PCa patients, which correlated with its tissue expression. Further investigation confirmed exosomal HOXD-AS1 promotes prostate cancer cell metastasis *in vitro* and *in vivo* by inducing metastasis associated phenotype. Mechanistically exosomal HOXD-AS1 was internalized directly by PCa cells, acting as competing endogenous RNA (ceRNA) to modulate the miR-361-5p/FOXM1 axis, therefore promoting PCa metastasis. In addition, we found that serum exosomal HOXD-AS1 was upregulated in metastatic PCa patients, especially those with high volume disease. And it is correlated closely with Gleason Score, distant and nodal metastasis, Prostatic specific antigen (PSA) recurrence free survival and progression free survival (PFS).

Conclusions: Our study sheds a new insight into the regulation of PCa distant metastasis by exosomal HOXD-AS1 mediated miR-361-5p/FOXM1 axis, and provided a promising liquid biopsy biomarker as well as therapeutic target to the detection and treatment of metastatic PCa.

Introduction

Prostate cancer (PCa) is the second commonly diagnosed malignancy and one of the leading cause of male cancer-related death worldwide[1]. Metastatic PCa is treated with either antiandrogen or chemotherapy regimens on the basis of androgen deprivation. Despite almost all patients respond to the initial treatment, disease progression is often inevitable after 18 ~ 24 months[2]. And it is the major cause of treatment failure and cancer death of PCa patients. However, the mechanism of PCa metastasis is not fully understood. Both selection and adaption theories are proposed to explain the progression and metastasis of PCa[3]. Accumulating evidence also support these theories that pre-existing castration resistant PCa cells, as well as adaptive genetic or epigenetic alteration under treatment pressure, concomitantly contribute to the metastasis of PCa[4, 5]. Recent studies also revealed that tumor

microenvironment (TME), which promotes the conversion of PCa cell phenotypes through various ways, plays important roles in the metastasis of PCa[6, 7]. However, the mechanism underlying how PCa cells acquire metastatic features during cancer evolving remains elusive. Identifying novel molecular mechanisms of how TME remold PCa phenotypes during metastasis holds great promise to improve the diagnosis and treatment of metastatic PCa.

Exosomes are membranous microvesicles ranging 40 ~ 150 nm in dimension, which are found in various human fluids including, but not limited to, blood, urine, and bile[8]. Recently, Tumor cell-derived exosomes are recognized as messengers that modulate local and systemic TME by transferring bioactive molecules such as proteins, RNAs, and DNAs[9]. Notably, long non-coding RNAs(lncRNAs) are identified as key molecular cargos of tumor cell-derived exosomes[10]. These functional lncRNAs transported by exosomes to a recipient cell can regulate tumor metastasis and progression by modulating downstream gene expression[11, 12]. For example, lncRNA-LNMAT2 transferred by bladder cancer cell derived exosomes upregulate *PROX1* expression, which promotes lymphangiogenesis and lymph nodes metastasis of bladder cancer[11]. Cancer associated fibroblasts promotes stemness and chemoresistance in colorectal cancer by delivering exosomal lncRNA-H19[12]. However, the biological function and mechanism of cancer cell-secreted exosomes in the distant metastasis of PCa remains unknown, warranting further exploration.

Previously we demonstrated that the lncRNA HOXD-AS1 is an important regulator in the progression of PCa by using two castration resistant prostate cancer (CRPC) cell models, LNCaP-AI and LNCaP-Bic[13]. Herein, we reported that HOXD-AS1 was found overexpressing in CRPC cell derived exosomes and serum exosomes from patients with PCa, which closely correlated with distant metastasis and survival. Functionally, Exosomal HOXD-AS1 promoted cellular migration *in vitro*, and distant metastasis of prostate cancer cell *in vivo*. Mechanistically, exosomal HOXD-AS1 was transferred directly to PCa cells, in which HOXD-AS1 served as competing endogenous RNA(ceRNA) by sponging miR-361-5p, which subsequently upregulated the expression of FOXM1, therefore facilitating metastasis. Our findings highlight the mechanism of exosomal HOXD-AS1 mediated transmitting of metastatic features in the PCa TME, and identified exosomal HOXD-AS1 as a potential marker of liquid biopsy and therapeutic target for metastasis in PCa.

Material And Methods

Cell culture

The cell lines used in this study were the human prostate cancer cells LNCaP and PC-3 (ATCC, Manassas, VA, USA), and the CRPC cell line LNCaP-Bic and LNCaP-AI as previously reported[13, 14]. LNCaP cells were cultured in RPMI-1640 (Gibco, Shanghai, China), supplemented with 10% FBS (fetal bovine serum, Shanghai ExCell Biology, China). PC-3 cells were cultured in F12-K supplemented with 10% FBS (Shanghai ExCell Biology, China). LNCaP-AI cells were cultured in phenol red free RPMI-1640 containing 10% charcoal stripped FBS (Gibco, Shanghai, China); whereas LNCaP-Bic were cultured with 20 μ M

bicalutamide (Sigma, St. Louis, MI, USA). All media were supplemented with 1% penicillin/streptomycin. Cells were grown in a humidified atmosphere of 5% CO₂ at 37°C.

Human tissue and serum samples

A total of 36 and 9 cases paraffin embedded PCa and benign prostate hypertrophy (BPH) tissues were obtained by surgery or needle biopsy, and 130 cases of serum samples were collected from treatment-naïve patients after their initial pathological diagnosis from the 1st Affiliated Hospital of Kunming Medical University. All the samples were pathologically diagnosed as prostate adenocarcinoma by two pathologists. The clinical features of the patients are listed in Table 1. The high volume and low volume in the metastatic patients were characterized according to the standard described in the CHAARTED trial[15]. All experiments were conducted with the approval of the Committees for Ethical Review of Research involving Human Subjects at the 1st Affiliated Hospital of Kunming Medical University. Informed consent was obtained from all participants prior to sample collection.

Isolation of cell derived exosomes and serum exosomes

LNCaP-AI and LNCaP-Bic cells were cultured for 48 hours in phenol-red free RPMI-1640 medium (Gibco) without supplements. Exosomes were isolated from the supernatant of CRPC cells by differential centrifugations as previously described[11]. Briefly, the medium was harvested and centrifuged at 300g for 10 min at 4°C. The supernatant was further centrifuged at 16500g for 20 min at 4°C and filtered through a 0.22µm filter. Exosomes were then pelleted by ultracentrifugation at 120,000g for 70 min at 4°C. Exosome pellets were resuspended in 0.22 µm-filtered PBS for subsequent experiments or stored at -80°C.

Exosomes were isolated from the human serum samples by Total Exosome Isolation kit (for serum) according to the manufacturer's instructions (ThermoFisher Scientific, USA). Briefly, serum samples were centrifuged at 2000g for 30 min at 4°C, then 200µl serum samples were mixed with 40µl Total Exosome Isolation reagent and incubated at 4°C for 1 hour. The mixtures were centrifuged at 10000g for 30 min at room temperature. Exosome pellets were resuspended in 50µl 0.2 µm-filtered PBS.

Transmission electron microscopy

Exosomes were adsorbed to a 400-mesh carbon-coated copper grids and stained with phosphotungstic acid. Morphologies of the samples were observed by a JEOL JEM-100SX transmission electron microscope (JEOL Ltd., Tokyo, Japan).

Nanoparticle tracking analysis

The number and size of the exosomes were directly tracked using the NS300 instrument (Malvern Instruments Ltd., Worcestershire, UK). The exosome pellets were resuspended and diluted in PBS to obtain a concentration within the recommended range ($1 \times 10^7 \sim 1 \times 10^9$ particles/mL). The samples were loaded into the sample chamber at ambient temperature. One 60s video was acquired for each sample.

The videos were then analyzed with the NTA3.2 software, which identified and tracked each particle's center under Brownian motion to measure the average distance the particles moved on a frame-by-frame basis.

Exosomes Tracking

Exosomes were stained with PKH67 Green Fluorescent Cell Linker Kit (Sigma Aldrich, St Louis, USA) according to the manufacturer's instruction. PKH67-labeled exosomes were collected by ultracentrifugation and resuspended in medium containing 10% exosome-depleted FBS. Then exosomes were added to PCa cells and incubated for 24 hours. Then cells were fixed with 4% formaldehyde after washing twice with PBS. The nuclei were stained with DAPI. A Zeiss confocal microscope was used to obtain the images.

RNA extraction and real-time quantitative PCR (qPCR) analysis

The experiments was conducted as previously described[16]. Total RNA from cells and exosomes was extracted using the TRIzol reagent (Life Technologies). RNA quantity was measured using a NanoDrop 2000 spectrophotometer (ThermoFisher Scientific). Total RNA was reverse transcribed by PrimeScript RT Master Mix (Takara Biotechnology Co., Ltd., Dalian, China). For miRNA reverse-transcription, Mir-X miRNA First-Strand Synthesis Kit (Takara Biotechnology Co., Ltd., Dalian, China) was used according to the manufacture's protocol. qRT-PCR analysis was conducted using the TBGreen II (Takara Biotechnology Co., Ltd.) and Mir-X miRNA qRT-PCR TB Green Kit (Takara Biotechnology Co., Ltd.), and analyzed on a Roche Light-Cycler 480 system (Roche, CA, USA). The relative gene expression was calculated using the $2^{-\Delta\Delta Ct}$ method. The transcription level of GAPDH was used as an internal control. All specific primers are listed in Additional file 1, Table S1.

Plasmid and miRNA Transfection and Lentivirus transduction

The pCDNA3.1-HOXD-AS1 overexpressing vector was constructed, and stable knockdown of HOXD-AS1 in PCa cells were obtained from our previous report[13]. The human hsa-miR-361-5p mimics was synthesize by GenePharma (GenePharma, Suzhou,China). The oligos used in knockdown and miRNA transfection was listed in Additional file 2, Table S2. The different segment of HOXD-AS1 was PCR-amplified from pCDNA3.1-HOXD-AS1 vector and cloned into psiCHECK2 luciferase vector (Promega, USA). The list of primers used in cloning reactions is presented in Additional file 3, Table S3. Transfection of miRNA and plasmids was performed using Lipofectamine 3000 (Life Technologies, USA).

Western Blot and antibodies

Western blotting was performed as previously described[17, 18]. Primary antibodies specific to E-Cadherin, Vimentin, GAPDH (1:1000, Cell Signaling Technology, MA, USA), TSG101, CD81, FOXM1 (1:1000, Abcam, Massachusetts, USA) were used. The blots were then incubated with goat anti-rabbit or

anti-mouse secondary antibody (Cell Signaling Technology, MA, USA) and visualized using enhanced chemiluminescence.

***In vitro* cell migration and wound-healing assays**

LNCaP and PC-3 were treated with CRPC-exos at 10 µg/ml in the functional assays. Transwell and Wound-healing assays were performed to detect cell migration. The details were described in our previous study[19, 20].

In situ hybridization (ISH)

HOXD-AS1 expression was examined using ISH in formalin-fixed, paraffin-embedded (FFPE) samples, as previously described[14]. The 5'-and 3'-DIG labeled HOXD-AS1 probe was synthesized by Sangon (Shanghai, China). The sequence was 5'- CGCATCTCTATTTGGTTTGA -3'. The staining intensity was graded as follows: 0 (no staining), 1 (weak staining, light brown), 2 (moderate staining, brown) and 3 (strong staining, deep brown). The intensity of staining was multiplied by the percentage of positive cells (0%-100%), and the H-score (0-300) of each tissue was obtained for statistical analysis. The score of ISH in the FFPE samples was blindly quantified by two pathologists and the average H-score (0-300) of each tissue was obtained for statistical analysis.

Luciferase Assay

5×10^4 cells were seeded in triplicate in 24-well plates and cultured for 24 hours and performed as previously described[14]. 250ng luciferase vectors and miRNA mimics at final concentration of 50 nmol/L were co-transfected by lipofectamine 3000. Luciferase and Renilla signals were measured 36 hours after transfection using the Dual Luciferase Reporter Assay Kit (Promega, USA) according to the manufacturer's protocol.

Animal Study

All mouse experiments were approved by the Institution of Animal Care and Use Committee of Kunming Medical University (approval No. KMMU2020213) and housed as previously reported[21]. For the bone metastasis study, PC-3-luc cells were pre-incubated with either PBS or CRPC-exos at a concentration 10 µg/ml in medium supplemented with exosome-depleted FBS for 48 hours (each group n=10). BALB/c-nu mice (4-week old, 18~20g) were anesthetized and the pre-treated cells were slowly inoculated into the left cardiac ventricle at 5×10^5 cells in 100 µL of PBS per mice. Then either PBS or 20µg indicated exosomes at 50µl volume were injected intra-cardiac under anesthesia weekly at the same time bioluminescence imaging was conducted. Osteolytic lesions were identified on radiographs as radiolucent lesions in the bone. Each bone metastasis was scored as previously reported[22] based on the following criteria: 0, no metastasis; 1, bone lesion <1/4 of the bone width; 2, bone lesion involving 1/4 to 1/2 of the bone width; 3, bone lesion over 1/2 to 3/4 of the bone width; and 4, bone lesion >3/4 of the bone width. The bone metastasis score for each mouse was the sum of the scores of all bone lesions from four limbs. For

survival studies, mice were monitored daily for signs of discomfort and were either euthanized all at one time or individually when presenting signs of distress, such as a 10% loss of body weight, or paralysis.

RIP assay

The RIP was performed as we described previously[16] using the EZ-Magna RIP kit (Millipore, USA). Ago2 and HA antibody (1:200, Abcam, Massachusetts, USA) were used. Normal rabbit IgG (provided with the kit) was used as a negative control.

Statistical analysis

Quantitative data were presented as the means \pm the standard deviation (SD) from three independent experiments. Differences between two groups were analyzed by the unpaired/paired Student's t test (two-tailed tests), and one-way ANOVA followed by

Dunnett's multiple comparisons tests was performed if more than two groups were compared. Data of clinical analysis were indicated as median with the interquartile range. The Mann-Whitney U test was applied for independent samples when the population could not be assumed to be normally distributed. Pearson's chi-square test was used to analyze the clinical variables. Spearman's correlation analysis was performed to determine the correlation between two variables. Cumulative survival time was calculated using the Kaplan-Meier method and analyzed by the log-rank test. A multivariate Cox proportional hazards model was used to estimate the adjusted hazard ratios and 95% confidence intervals, and to identify independent prognostic factors. All statistical analysis in this study were performed using SPSS 19.0 software. A P value<0.05 was considered significant.

Results

HOXD-AS1 is overexpressed in CRPC cell-derived and PCa patients' serum exosomes.

In our previous study, two CRPC cell lines were established, and we found that lncRNA HOXD-AS1 is overexpressed in these cell lines and exerts key regulatory role in the castration resistance of PCa[13]. Interestingly, we found that the motility of PCa cell LNCaP and PC-3 was enhanced significantly when cultured with CRPC cell-conditioned medium (Fig. 1A-B). Recent study recognized that exosomes are the important vehicles in the inter-cellular communication. Then we isolated exosomes from cultural medium of PCa cells and found that HOXD-AS1 was significantly overexpressed in the CRPC cell derived exosomes (CRPC-exos), as compared with those from LNCaP and PC-3(Fig. 1C). Additionally, we also noticed that HOXD-AS1 was highly enriched in CRPC-exos than that of cellular expression, but not normal PCa cells and its exosomes (Fig. 1D). As a result, we propose that during PCa progression, HOXD-AS1 may be transmitted from CRPC cells to normal PCa cells through exosomes, as according to the selection and adaption theory[3]. Next, we asked whether cancer cell derived exosomes also existed in PCa patients. RNA in-situ hybridization found that HOXD-AS1 was overexpressed in metastatic PCa specimens (Fig. 1E-F), as consistent with our previous findings from TCGA and GEO datasets [13].

Notably, extra-cellular expression of HOXD-AS1 was also observed, further indicating the existence of exosomal HOXD-AS1 in clinical specimens (Fig. 1E). Moreover, HOXD-AS1 was also detectable in serum exosomes from PCa patients, and was significantly upregulated in metastatic PCa patients (Fig. 1G). Interestingly, we also noticed that HOXD-AS1 expression in serum exosomes was closely correlated with its tissue expression in PCa patients (Fig. 1G, $r=0.57$, $P<0.01$). Collectively, these findings clearly indicate that CRPC cell secreted exosomes HOXD-AS1 may participated in the metastasis of PCa.

CRPC cell derived exosomes promotes PCa cell migration *in vitro* by inducing metastasis associated phenotype.

First of all, we sought to characterized the exosomes secreted by CRPC cells. Exosomes derived by LNCaP-AI and LNCaP-Bic cells was isolated from cultural medium. We found that exosomes with an 80-150 nm in size and a typical cup-shaped morphology were detected by NanoSight analysis (NTA) (Fig. 2A) and transmission electron microscopy (TEM) (Fig. 2B). Then we detected exosomal protein markers CD81 and TSG101 by Western Blot and found that these markers were detectable from both cell lysate and exosomes, but not the supernant of cultural medium. This result further confirmed that the particles enriched from the culture medium were exosomes (Fig. 2C). Consistent with our findings, CRPC-exos also significantly enhanced the migration of PCa cells, as measured by transwell assay (Fig. 2D-E). Furthermore, CRPC-exos significantly accelerated the speed of wound healing in LNCaP and PC-3 cells, indicating an increased cellular motility (Fig. 2F-I). Additionally, we also investigated if this phenomenon was associated with epithelial to mesenchymal transition (EMT), one of the most important changes during cancer metastasis. As expected, we confirmed that the epithelial marker E-Cadherin was downregulated, while the mesenchymal marker Vimentin was upregulated after PCa cells were treated with CRPC-exos for 48 hours (Fig. 2J-K), as detected by both qPCR and Western Blot. Above all, our data demonstrate that CRPC cell secreted exosomes promoted migration of PCa *in vitro* by inducing metastatic phenotype of the PCa cells.

CRPC derived exosome enhances PCa cell motility by delivering HOXD-AS1.

As we observed that CRPC-exos strongly increased the migration of PCa cells. We then tried to investigate whether this biological function was achieved through transferring of HOXD-AS1 by exosomes. First of all, we evaluated the internalization of CRPC-exos by PCa cells. We labeled purified exosomes with PKH67 green fluorescent dye and incubated them with LNCaP and PC-3 for 24 hours. Confocal images showed the green fluorescent punctate signal in the cytoplasm of recipient PCa cells, indicating internalization of the PKH67-labeled exosomes. By contrast, no PKH67 fluorescent signal was observed in the control group, suggesting that the PCa cells specifically internalized the CRPC cell-secreted exosomes (Fig. 3A). We further examined whether exosomal HOXD-AS1 was successfully transferred to the PCa cells and found that HOXD-AS1 expression was significantly elevated in LNCaP and PC-3 cells after incubation with the CRPC-exos (Fig. 3B). Moreover, HOXD-AS1 knockdown in LNCaP-AI and LNCaP-Bic cells led to a significant reduced (Fig. 3C), while HOXD-AS1 overexpression resulted in an increased HOXD-AS1 expression in CRPC-exos (Additional file 4: Fig. S1A). Furthermore, exosomes from HOXD-AS1

knockdown CRPC cells failed to enhance HOXD-AS1 expression when treated to normal PCa cells (Additional file 4: Fig. S1B-C). As a consequence, HOXD-AS1 knockdown in CRPC-exos diminished its ability of increasing PCa cell migration, as measured by transwell assay (Fig. 3D-E). Similarly, the speed of wound healing was significantly reduced when treated with HOXD-AS1 knockdown exosomes, as compared with control CRPC-exos (Fig. 3F-G, Additional file 4: Fig. S1D-E). Taken together, our data demonstrated that CRPC-exos promoted the motility of PCa cells by specifically transmitting HOXD-AS1.

Exosomal HOXD-AS1 promotes distant metastasis of PCa *in vivo*.

To further explore the function of exosomal HOXD-AS1 in the metastasis of PCa, we applied a mouse model of bone metastasis, which is the most common distant metastatic site in PCa patients. First of all, luciferase-expressing PC-3 cells were pre-treated with either PBS or CRPC-exos, HOXD-AS1 knockdown CRPC-exos or its control for 48 hours and then inoculated into the left cardiac ventricle of male nude mice to monitor the development of bone metastasis. After the inoculation, respective exosomes were injected intra-cardiac weekly to ensure a constant effect of exosomes on PCa cells. Surprisingly, CRPC-exos strongly promoted the formation of bone metastasis compared with the control group, as detected by bioluminescence imaging (Fig. 4A-B). By contrast, the pro-metastasis feature of CRPC-exos was significantly diminished by HOXD-AS1 (Fig. 4A-B). The bone metastasis was further confirmed by X-ray imaging, indicating a significantly worse destruction of cortical bone and higher bone score in the CRPC-exos and CRPC-exos control group (Fig. 4C-D). Meanwhile, we also observed a significantly shortened metastatic-free survival in the CRPC-exos and CRPC-exos control group, as compared with PBS and HOXD-AS1 knockdown exosomes, respectively (Fig. 4E). Additionally, we also conducted H&E staining on the bone tissue sections. An increased bone metastasis burden and more extensive osteolytic lesions was observed in the CRPC-exo treated group, as compared with control (Fig. 1F). Consistently, significantly less metastatic tumor and osteolytic lesions were observed in the group using HOXD-AS1 knockdown exosomes. Collectively, our results supported that CRPC cell derived exosomal HOXD-AS1 promoted the distant metastasis of PCa *in vivo*.

Exosomal HOXD-AS1 promotes PCa metastasis via miR-361-5p/FOXO1 axis

Considering our find that CRPC-exos was internalized in the cytoplasm, and most exosomal lncRNA act as competing endogenous RNA (ceRNA), we sought to investigate whether exosomal HOXD-AS1 function as RNA sponge in PCa cells. Interestingly, as one of the most enriched microRNA in PCa, the expression of miR-361-5p was negatively correlated with HOXD-AS1 ($R=-0.21$, $P<0.01$), as analyzed by Starbase database (Fig. 5A)[23]. Moreover, miR-361-5p is reported as an important tumor suppressor in various types of cancer, including prostate, breast and lung[24-26]. Notably, miR-361-5p was reported to inhibit metastasis through inhibiting EMT in prostate cancer[27]. So we proposed that exosomal HOXD-AS1 may interacted with miR-361-5p after it was internalized in PCa cells. To test our hypothesis, we treated LNCaP and PC-3 cells with CRPC secreted exosomes and found that the expression of miR-361-5p was significantly downregulated, accompanied by the upregulation of HOXD-AS1 (Fig. 5B). Similar with the effect of CRPC-exos, overexpression of HOXD-AS1 inhibited the expression (Additional file 5: Fig. S2A),

while downregulation of HOXD-AS1 by lentivirus upregulated miR-361-5p in PCa cells (Additional file 5: Fig. S2B). On the other hand, exosomes from HOXD-AS1 knockdown CRPC cells were not able to inhibit the expression of miR-361-5p (Fig. 5C). Furthermore, by searching miRanda and CLIP-seq data from Starbase[23], we identified a potential binding site at 983~1006nt of HOXD-AS1 with miR-361-5p (Fig. 5D). And psiCHECK2 vector containing different truncated segment of HOXD-AS1 was generated, then luciferase assay was carried out to identify the region of HOXD-AS1 binding with miR-361-5p. Consistent with bioinformatic prediction, we found that the luciferase activity was significantly inhibited with the segment containing HOXD-AS1 983~1006nt, but not other regions (Fig. 5E). Next, vector containing site-directed mutagenesis of miR-361-5p binding site was constructed (Fig. 5F). MiR-361-5p significantly inhibited the luciferase activity of the vector containing wild-type HOXD-AS1 fragment, but not the mutant vector (Fig. 5G). Additionally, we performed an RNA immunoprecipitation (RIP) and found a significant enrichment of both HOXD-AS1 and miR-361-5p by Ago2 antibody compared with IgG (Fig. 5H-I). Besides, vectors expressing Ago2 with HA tag was transfected into 293T cells and RIP was also conducted by HA antibody. Similarly, HOXD-AS1 and miR-361-5p was able to be enriched by exogenous Ago2 (Fig. 5H and J), which further supported their specific interaction. Last but not least, we detected the expression of *FOXM1*, a key modulator in prostate cancer progression and metastasis, as well as the most reported miR-361-5p target[26, 28]. As a result, *FOXM1* expression was significantly inhibited by miR-361-5p transfection in both LNCaP and PC-3 cells, as detected by Western Blot (Fig. 5K). CRPC-exos significantly increased the expression of *FOXM1* in PCa cells, while overexpression of miR-361-5p reversed its effect (Fig. 5L). Taken together, our data clearly demonstrated that exosomal HOXD-AS1 function as an ceRNA sponging miR-361-5p, which in turn upregulated the expression of *FOXM1* in PCa cells, therefore promoting distant metastasis.

Serum exosomal HOXD-AS1 expression associates with clinical characteristics and prognosis in PCa.

As we found that exosomal HOXD-AS1 was detectable in the serum exosomes in PCa patients, and correlated with tissue expression, we asked whether exosomal HOXD-AS1 expression correlates with clinical characteristics and prognosis. Firstly, we isolated exosomes from the serum of treatment-naïve PCa patients and characterized its features. Similar with our findings from cellular exosomes, serum exosomes displayed cup-shaped morphology with a dimension ranging from 80~150nm, as measured by TEM and NTA (Fig. 6A-B). It also expressed exosomal markers CD81 and TSG101, as detected by Western Blot (Fig. 6C). Secondly, we isolated the serum exosomes of a PCa cohort with 130 patients before their initial treatment and detected the expression of HOXD-AS1 by qPCR. Serum exosomal HOXD-AS1 was significantly elevated in metastatic PCa patients, as compared with localized disease (Fig. 6D). Interestingly, the expression of serum exosomal HOXD-AS1 was much more obviously increased in M1 patients with high metastatic volume compared with either low volume or localized disease (Fig. 6E). Besides, serum exosomal HOXD-AS1 expression was also significantly upregulated in PCa patients with positive nodal metastasis and higher Gleason Score (Fig. 6F-G), but not tumor stage (Additional file 6: Fig. S3). Meanwhile, serum exosomal HOXD-AS1 level was significantly correlated with the Gleason Score, lymph node and metastatic status of PCa patients (Table 1). Receiver operating characteristic (ROC) analysis showed that serum exosomal HOXD-AS1 could discriminate between patients with

metastasis and localized controls, and there was higher diagnostic accuracy, as measured by the area under the curve (AUC), for diagnosing distant metastasis in PCa (Fig. 6H). Since we found that serum exosomal HOXD-AS1 was elevated significantly in metastatic PCa and closely correlated with distant metastasis, we explored whether its expression is associated with prognosis of metastatic PCa patients. Survival analysis showed that high exosomal HOXD-AS1 expression PCa patients had a significantly shorter PSA recurrence-free survival (PRFS) and progression-free survival (PFS) ($P=0.006$, HR=2.05, 1.24~3.38; $P=0.02$, HR=2.27, 1.00~5.14, respectively. Fig. 6I-J). Additionally, Univariate and multivariate analysis revealed that serum exosomal HOXD-AS1 expression together with tumor stage was prognostic factor for PRFS in PCa patients (Table 2), and an independent prognostic factor for PFS (Additional file 7: Table S4). Collectively, these findings suggest that serum exosomal HOXD-AS1 expression correlated closely with clinical features in PCa patients, and could be applied as a potential bio-marker for diagnosing and predicting the prognosis for metastatic PCa.

Discussion

Metastasis is the major cause of PCa-related death[29]. Despite androgen deprivation based novel therapies has improved the prognosis of metastatic PCa, the 5-year overall survival rate is around 30.5% compared with over 90% in patient with localized disease[29, 30]. Although it has been reported that cellular communication by direct contact, hormones and metabolites in the TME participates in cancer metastasis, the significance of cellular interaction by exosomal lncRNA in PCa remains unknown. Herein, we demonstrated that a CRPC cell secreted exosomal lncRNA HOXD-AS1 is involved in the metastasis of PCa. Exosomal HOXD-AS1 was internalized by normal PCa cells, enhanced cellular motility by inducing metastatic phenotype *in vitro* and promoted distant metastasis *in vivo*. Mechanistically, exosomal HOXD-AS1 act as ceRNA to specifically bind with miR-361-5p, which subsequently upregulated the expression its target FOXM1, resulting in the metastasis of PCa. Additionally, we also demonstrated that serum exosomal HOXD-AS1 was elevated in metastatic patients and could be used as a marker for diagnosis and predicting the prognosis for metastatic PCa. These findings provided in-depth mechanistic and translational insights into the axis by which exosomal HOXD-AS1 promotes PCa metastasis, and that it may emerge as a novel marker for liquid biopsy and therapeutic target in PCa.

Exosomes have been studied for their role in intercellular communication in the TME. Previously, several studies have revealed that exosomal lncRNAs were involved in the proliferation, therapeutic resistance, and metastasis in various cancers, and its biological effect is achieved by direct transferring RNA to the recipient cells[12, 31, 32]. Herein, we found that HOXD-AS1 was overexpressed in CRPC cell derived exosomes and serum exosomes from metastatic PCa patient. Further exploration revealed that CRPC-exos was directly internalized into PCa cells, thus facilitating transmitting HOXD-AS1 from CRPC cells to normal PCa cells in the TME. Functionally, exosomal HOXD-AS1 significantly enhanced the motility of PCa cells by inducing EMT. Notably, *in vivo* study revealed that CRPC-exos strongly promoted bone metastasis, the most common type of distant metastasis of PCa. Our results showed that exosomal HOXD-AS1 promoted metastasis of PCa, suggesting that it may represent a potential target for clinical intervention in PCa patients with distant metastasis.

It is well established that most lncRNAs transmitted by exosomes located at the cytoplasm of the recipient, function as ceRNA to bind with miRNAs, which subsequently facilitate target gene expression[10]. HOXD-AS1 has been well characterized as a ceRNA to modulate progression in a variety of cancers, including glioma [33], hepatocellular carcinoma [34] and cervical cancer[35]. However, its role as exosomal lncRNA in PCa cells remains unclear. Despite the fact that we previously reported that HOXD-AS1 is distributed both in the cytoplasm and nucleus, and nucleic HOXD-AS1 act as a molecular scaffold to mediate gene transcription [13], its function in the cytoplasm is elusive. In the present study, we identified exosomal HOXD-AS1 directly interacted with miR-361-5p, one of the most enriched miRNAs in PCa. Importantly, miR-361-5p is downregulated in CRPC and represses PCa progression by directly inhibit its downstream target expression [24, 27]. Moreover, miR-361-5p is also a key tumor suppressor many types of cancers[25, 26], which could inhibit tumor metastasis through different mechanisms[25, 36], including repressing EMT[26, 37]. Last but not least, FOXM1, as one of the most important oncogene in PCa as well as the direct target of miR-361-5p[26, 38], was revealed as the target of exosomal HOXD-AS1 in our current study. Therefore, our research provided that exosomal HOXD-AS1 act as a ceRNA that binding with miR-361-5p, facilitating its target FOXM1 expression therefore promoting PCa metastasis, which expanded current knowledge on HOXD-AS1 regulation in PCa.

Another important finding in the present study was that we proposed a novel aspect to support the co-existence of adaption and selection models in PCa progression and metastasis. Initially, these two models were proposed to explain the progression of PCa and thought to be mutually exclusive[2, 3, 39–41]. However, recent studies using more sophisticated models or techniques demonstrated that these two models co-exist and work dependently during the initiation and progression of PCa [42, 43]. Pre-existing therapeutic-resistant PCa cells are identified with unique gene expression signatures, which could be convertible during PCa progression[43–45]. In our present study, we identified that CRPC cell secreted exosome could promote the migration of PCa cells *in vitro* and *in vivo* by transmitting HOXD-AS1. Acquired exosomal HOXD-AS1 in normal PCa cells triggered metastatic signaling by regulating the miR-361-5p/FOXM1 axis. Our findings supported the theories that both pre-existing CRPC cells and acquired epigenetic changes could contribute to the metastasis of PCa. Common PCa cells could be converted into more aggressive types with metastatic features, in a novel pathway of intercellular communication mediated by exosomal lncRNA.

Exosomal RNAs are emerging as novel diagnostic bio-makers for its non-invasiveness and stable in body fluids[46]. Exosomal androgen receptor splice variant 7 (*AR-V7*) detection has been applied clinically as the marker to predict the sensitivity of novel anti-androgen regimens[47]. Moreover, Exosomal microRNAs and lncRNAs are also reported as useful markers for diagnosing PCa[48–50]. Herein, we found that HOXD-AS1 was overexpressed in serum exosomes from patients with metastatic PCa, and it was positively associated with nodal and distant metastasis. Importantly, the efficacy of serum exosomal HOXD-AS1 as bio-marker for metastatic PCa diagnosis and prognosis was evaluated, and we found that it was closely correlated with significantly worse PRFS and PFS. The results indicated that exosomal HOXD-AS1 analysis could be utilized for early detection of metastasis, and predicting the prognosis of metastatic PCa patients even before their first treatment.

Conclusions

In summary, our findings revealed evidence of the mechanism in which CRPC cell-derived exosomal HOXD-AS1 promoted PCa metastasis by modulating miR-361-5p/FOXM1 axis. We also reported that serum exosomal HOXD-AS1 detection could be applied as a marker for metastatic disease, as well as predicting the prognosis of PCa patients. Our study not only identifies a crucial mechanism of exosomal lncRNA-mediated intercellular communication from CRPC cells to the TME, which endowed common PCa cell with metastatic features, but also develops a potential non-invasive diagnostic approach for PCa.

Abbreviations

PCa: Prostate cancer, CRPC: Castration resistance prostate cancer, lncRNA: Long noncoding RNA, TME: Tumor microenvironment, PSA: Prostatic specific antigen, BPH: benign prostate hypertrophy, ceRNA: competing endogenous RNA, EMT: Epithelial to mesenchymal transition, FOXM1: Forkhead box M1, qPCR: quantitative polymerase chain reaction, ISH: *in situ* hybridization, PRFS: prostatic specific antigen recurrence-free survival, PFS: progression-free survival, RIP: RNA immunoprecipitation, FFPE: Formalin-fixed, paraffin-embedded, GAPDH: Glyceraldehyde-3-phosphate dehydrogenase, NTA: NanoSight analysis, TEM: transmission electron microscopy.

Declarations

Ethics approval and consent to participate

We obtained human prostate samples by surgery or needle biopsy, and serum samples with the written consent of patients who underwent treatment at The 1st Affiliated Hospital of Kunming Medical University. Ethical consent was approved by The 1st Affiliated Hospital of Kunming Medical University's Committees for Ethical Review of Research involving Human Subjects.

Consent for Publication

All authors have read and approved the final manuscript for publication.

Availability of data and material

The primary data from microarray analysis have been deposited to the Gene Expression Omnibus and the accession numbers is GSE93929. The rest of the data used and analyzed during the current study are available from the corresponding author on reasonable request.

Competing interests

The authors declare that they have no conflict of interests.

Funding

This study was supported by the National Natural Science Foundation of China (Grant No. 81802548, 81860451), Yunnan Natural Science Foundation (Grant No. 202001AW070001), Yunnan Health Training Project of High-Level Talents (for Peng Gu, Grant No. H2018070), Provincial Natural Science Foundation of Yunnan-Kunming Medical University Joint Foundation (Grant No. 2019FE001-136), Scientific Research Project of Yunnan Provincial Educational Department (Grant No. 2018JS208). Funding for young doctors (for Peng Gu), from the 1st Affiliated Hospital of Kunming Medical University (Grant No. 2017BS016).

Author Contributions

X.L. and P.G. designed the study, analyzed data, and wrote the manuscript. Y.J., P.G. and H.Z. performed the initial experimental design, participated in the experiment, performed data analysis, and wrote the initial manuscript. Y.C., T.L. and K.L. performed the animal experiments, migration assays and RNA-ISH, B.Z. analyzed the clinical data. L.Q. and J.S. performed vector constructing, luciferase assays and RIP assays.

Acknowledgements

We thank Prof. Yun Zhang and Prof. Wenhui Lee from Kunming Institute of Zoology, China Academy of Science, for their experimental facilities and suggestions during our research.

References

1. Sung H, Ferlay J, Siegel RL, Laversanne M, Soerjomataram I, Jemal A, et al: Global cancer statistics 2020: GLOBOCAN estimates of incidence and mortality worldwide for 36 cancers in 185 countries. *CA Cancer J Clin* 2021.
2. Katzenwadel A, Wolf P: Androgen deprivation of prostate cancer: Leading to a therapeutic dead end. *Cancer Lett* 2015, 367:12-17.
3. Zong Y, Goldstein AS: Adaptation or selection—mechanisms of castration-resistant prostate cancer. *Nat Rev Urol* 2013, 10:90-98.
4. Mevel R, Steiner I, Mason S, Galbraith LC, Patel R, Fadlullah MZ, et al: RUNX1 marks a luminal castration-resistant lineage established at the onset of prostate development. *Elife* 2020, 9.
5. Esposito M, Fang C, Cook KC, Park N, Wei Y, Spadazzi C, et al: TGF-beta-induced DACT1 biomolecular condensates repress Wnt signalling to promote bone metastasis. *Nat Cell Biol* 2021, 23:257-267.
6. Quintanal-Villalonga A, Chan JM, Yu HA, Pe'er D, Sawyers CL, Sen T, et al: Lineage plasticity in cancer: a shared pathway of therapeutic resistance. *Nat Rev Clin Oncol* 2020, 17:360-371.
7. Huang R, Wang S, Wang N, Zheng Y, Zhou J, Yang B, et al: CCL5 derived from tumor-associated macrophages promotes prostate cancer stem cells and metastasis via activating beta-catenin/STAT3 signaling. *Cell Death Dis* 2020, 11:234.
8. Kalluri R: The biology and function of exosomes in cancer. *J Clin Invest* 2016, 126:1208-1215.

9. Aheget H, Mazini L, Martin F, Belqat B, Marchal JA, Benabdellah K: Exosomes: Their Role in Pathogenesis, Diagnosis and Treatment of Diseases. *Cancers (Basel)* 2020, 13.
10. Pathania AS, Challagundla KB: Exosomal Long Non-coding RNAs: Emerging Players in the Tumor Microenvironment. *Mol Ther Nucleic Acids* 2021, 23:1371-1383.
11. Chen C, Luo Y, He W, Zhao Y, Kong Y, Liu H, et al: Exosomal long noncoding RNA LNMAT2 promotes lymphatic metastasis in bladder cancer. *J Clin Invest* 2020, 130:404-421.
12. Ren J, Ding L, Zhang D, Shi G, Xu Q, Shen S, et al: Carcinoma-associated fibroblasts promote the stemness and chemoresistance of colorectal cancer by transferring exosomal lncRNA H19. *Theranostics* 2018, 8:3932-3948.
13. Gu P, Chen X, Xie R, Han J, Xie W, Wang B, et al: lncRNA HOXD-AS1 Regulates Proliferation and Chemo-Resistance of Castration-Resistant Prostate Cancer via Recruiting WDR5. *Mol Ther* 2017, 25:1959-1973.
14. Gu P, Chen X, Xie R, Xie W, Huang L, Dong W, et al: A novel AR translational regulator lncRNA LBCS inhibits castration resistance of prostate cancer. *Mol Cancer* 2019, 18:109.
15. Sweeney CJ, Chen YH, Carducci M, Liu G, Jarrard DF, Eisenberger M, et al: Chemohormonal Therapy in Metastatic Hormone-Sensitive Prostate Cancer. *N Engl J Med* 2015, 373:737-746.
16. Chen X, Xie R, Gu P, Huang M, Han J, Dong W, et al: Long noncoding RNA LBCS inhibits self-renewal and chemoresistance of bladder cancer stem cells through epigenetic silencing of SOX2. *Clin Cancer Res* 2018.
17. Chen X, Gu P, Xie R, Han J, Liu H, Wang B, et al: Heterogeneous nuclear ribonucleoprotein K is associated with poor prognosis and regulates proliferation and apoptosis in bladder cancer. *J Cell Mol Med* 2017, 21:1266-1279.
18. Chen Z, Chen X, Xie R, Huang M, Dong W, Han J, et al: DANCR Promotes Metastasis and Proliferation in Bladder Cancer Cells by Enhancing IL-11-STAT3 Signaling and CCND1 Expression. *Mol Ther* 2019, 27:326-341.
19. Jiang J, Chen X, Liu H, Shao J, Xie R, Gu P, et al: Polypyrimidine Tract-Binding Protein 1 promotes proliferation, migration and invasion in clear-cell renal cell carcinoma by regulating alternative splicing of PKM. *Am J Cancer Res* 2017, 7:245-259.
20. Xie R, Chen X, Chen Z, Huang M, Dong W, Gu P, et al: Polypyrimidine tract binding protein 1 promotes lymphatic metastasis and proliferation of bladder cancer via alternative splicing of MEIS2 and PKM. *Cancer Lett* 2019, 449:31-44.
21. Chen X, Xie W, Gu P, Cai Q, Wang B, Xie Y, et al: Upregulated WDR5 promotes proliferation, self-renewal and chemoresistance in bladder cancer via mediating H3K4 trimethylation. *Sci Rep* 2015, 5:8293.
22. Wa Q, Huang S, Pan J, Tang Y, He S, Fu X, et al: miR-204-5p Represses Bone Metastasis via Inactivating NF-kappaB Signaling in Prostate Cancer. *Mol Ther Nucleic Acids* 2019, 18:567-579.
23. Li JH, Liu S, Zhou H, Qu LH, Yang JH: starBase v2.0: decoding miRNA-ceRNA, miRNA-ncRNA and protein-RNA interaction networks from large-scale CLIP-Seq data. *Nucleic Acids Res* 2014, 42:D92-97.

24. Liu D, Tao T, Xu B, Chen S, Liu C, Zhang L, et al: MiR-361-5p acts as a tumor suppressor in prostate cancer by targeting signal transducer and activator of transcription-6(STAT6). *Biochem Biophys Res Commun* 2014, 445:151-156.
25. Ma F, Zhang L, Ma L, Zhang Y, Zhang J, Guo B: MiR-361-5p inhibits glycolytic metabolism, proliferation and invasion of breast cancer by targeting FGFR1 and MMP-1. *J Exp Clin Cancer Res* 2017, 36:158.
26. Hou XW, Sun X, Yu Y, Zhao HM, Yang ZJ, Wang X, et al: miR-361-5p suppresses lung cancer cell lines progression by targeting FOXM1. *Neoplasma* 2017, 64:526-534.
27. Ling Z, Liu D, Zhang G, Liang Q, Xiang P, Xu Y, et al: miR-361-5p modulates metabolism and autophagy via the Sp1-mediated regulation of PKM2 in prostate cancer. *Oncol Rep* 2017, 38:1621-1628.
28. Zhang L, Li B, Zhang B, Zhang H, Suo J: miR-361 enhances sensitivity to 5-fluorouracil by targeting the FOXM1-ABCC5/10 signaling pathway in colorectal cancer. *Oncol Lett* 2019, 18:4064-4073.
29. Qi JL, Wang LJ, Zhou MG, Liu YN, Liu JM, Liu SW, et al: [Disease burden of prostate cancer among men in China, from 1990 to 2013]. *Zhonghua Liu Xing Bing Xue Za Zhi* 2016, 37:778-782.
30. Litwin MS, Tan HJ: The Diagnosis and Treatment of Prostate Cancer: A Review. *JAMA* 2017, 317:2532-2542.
31. Fan Q, Yang L, Zhang X, Peng X, Wei S, Su D, et al: The emerging role of exosome-derived non-coding RNAs in cancer biology. *Cancer Lett* 2018, 414:107-115.
32. Qu L, Ding J, Chen C, Wu ZJ, Liu B, Gao Y, et al: Exosome-Transmitted lncARSR Promotes Sunitinib Resistance in Renal Cancer by Acting as a Competing Endogenous RNA. *Cancer Cell* 2016, 29:653-668.
33. Chen Y, Zhao F, Cui D, Jiang R, Chen J, Huang Q, et al: HOXD-AS1/miR-130a sponge regulates glioma development by targeting E2F8. *Int J Cancer* 2018, 142:2313-2322.
34. Lu S, Zhou J, Sun Y, Li N, Miao M, Jiao B, et al: The noncoding RNA HOXD-AS1 is a critical regulator of the metastasis and apoptosis phenotype in human hepatocellular carcinoma. *Mol Cancer* 2017, 16:125.
35. Chen S, Li K: HOXD-AS1 facilitates cell migration and invasion as an oncogenic lncRNA by competitively binding to miR-877-3p and upregulating FGF2 in human cervical cancer. *BMC Cancer* 2020, 20:924.
36. Ma J, Jing X, Chen Z, Duan Z, Zhang Y: MiR-361-5p decreases the tumorigenicity of epithelial ovarian cancer cells by targeting at RPL22L1 and c-Met signaling. *Int J Clin Exp Pathol* 2018, 11:2588-2596.
37. Tian L, Zhao Z, Xie L, Zhu J: MiR-361-5p inhibits the mobility of gastric cancer cells through suppressing epithelial-mesenchymal transition via the Wnt/beta-catenin pathway. *Gene* 2018, 675:102-109.
38. Shen B, Zhou N, Hu T, Zhao W, Wu D, Wang S: LncRNA MEG3 negatively modified osteosarcoma development through regulation of miR-361-5p and FoxM1. *J Cell Physiol* 2019, 234:13464-13480.

39. Mousses S, Wagner U, Chen Y, Kim JW, Bubendorf L, Bittner M, et al: Failure of hormone therapy in prostate cancer involves systematic restoration of androgen responsive genes and activation of rapamycin sensitive signaling. *Oncogene* 2001, 20:6718-6723.
40. Craft N, Chhor C, Tran C, Beldegrun A, DeKernion J, Witte ON, et al: Evidence for clonal outgrowth of androgen-independent prostate cancer cells from androgen-dependent tumors through a two-step process. *Cancer Res* 1999, 59:5030-5036.
41. Goldstein AS, Huang J, Guo C, Garraway IP, Witte ON: Identification of a cell of origin for human prostate cancer. *Science* 2010, 329:568-571.
42. Schnepf PM, Shelley G, Dai J, Wakim N, Jiang H, Mizokami A, et al: Single-Cell Transcriptomics Analysis Identifies Nuclear Protein 1 as a Regulator of Docetaxel Resistance in Prostate Cancer Cells. *Mol Cancer Res* 2020, 18:1290-1301.
43. Dong B, Miao J, Wang Y, Luo W, Ji Z, Lai H, et al: Single-cell analysis supports a luminal-neuroendocrine transdifferentiation in human prostate cancer. *Commun Biol* 2020, 3:778.
44. Chen S, Zhu G, Yang Y, Wang F, Xiao YT, Zhang N, et al: Single-cell analysis reveals transcriptomic remodellings in distinct cell types that contribute to human prostate cancer progression. *Nat Cell Biol* 2021, 23:87-98.
45. Chakraborty G, Armenia J, Mazzu YZ, Nandakumar S, Stopsack KH, Atiq MO, et al: Significance of BRCA2 and RB1 Co-loss in Aggressive Prostate Cancer Progression. *Clin Cancer Res* 2020, 26:2047-2064.
46. Yu W, Hurley J, Roberts D, Chakraborty SK, Enderle D, Noerholm M, et al: Exosome-based liquid biopsies in cancer: opportunities and challenges. *Ann Oncol* 2021, 32:466-477.
47. Del Re M, Biasco E, Crucitta S, Derosa L, Rofi E, Orlandini C, et al: The Detection of Androgen Receptor Splice Variant 7 in Plasma-derived Exosomal RNA Strongly Predicts Resistance to Hormonal Therapy in Metastatic Prostate Cancer Patients. *Eur Urol* 2017, 71:680-687.
48. Kohaar I, Chen Y, Banerjee S, Borbiev T, Kuo HC, Ali A, et al: A Urine Exosome Gene Expression Panel Distinguishes between Indolent and Aggressive Prostate Cancers at Biopsy. *J Urol* 2021, 205:420-425.
49. Isin M, Uysaler E, Ozgur E, Koseoglu H, Sanli O, Yucel OB, et al: Exosomal lncRNA-p21 levels may help to distinguish prostate cancer from benign disease. *Front Genet* 2015, 6:168.
50. Fredsoe J, Rasmussen AKI, Mouritzen P, Borre M, Orntoft T, Sorensen KD: A five-microRNA model (pCaP) for predicting prostate cancer aggressiveness using cell-free urine. *Int J Cancer* 2019, 145:2558-2567.

Tables

Table 1. Association between serum exosomal HOXD-AS1 expression and clinicopathological features of prostate cancer patients.

Characteristics	Cases(%)		χ^2	P-value
Total Patients(N)	130			
Exosomal HOXD-AS1 expression	Low	High		
Age(Year)				
≤70	38(29)	31(24)	1.513	0.219
>70	27(21)	34(26)		
Gleason Score				
6-7	37(28)	28(22)	11.377	0.001*
8-10	28(22)	37(28)		
Tumor stage				
T2	41(31)	30(23)	3.755	0.053
T3-4	24(19)	35(27)		
Lymphnodes status N				
Negative	59(45)	40(31)	15.292	0.000*
Positive	6(5)	25(19)		
Distant Metastasis M				
M0	30(23)	8(6)	17.998	0.000*
M1	35(27)	57(44)		

* $P < 0.05$ is considered significant.

Median serum exosomal HOXD-AS1 expression was used as cut-off value for analysis

Table 2. Univariate and multivariate analysis of factors associated with PSA recurrence-free survival in metastatic prostate cancer cohort.

Variable	Univariate			Multivariate		
	HR	95% CI	<i>p</i>	HR	95% CI	<i>p</i>
Age, years (>70/≤70)	1.455	0.886–2.389	0.138			NA
Gleason Score (8-10/6-7)	1.543	0.863-2.759	0.140			
Tumor stage (T3-4/T1-2)	2.381	1.430-3.967	0.001	2.056	1.215-3.479	0.007
Nodal metastasis (N1/N0)	1.361	0.796-2.326	0.260			NA
Exosomal HOXD-AS1 (high/low)	2.224	1.332-3.714	0.002	1.873	1.104-3.178	0.020

Univariate and multivariate analysis. Cox proportional hazards regression model. Variables associated with survival by univariate analyses were adopted as covariates in multivariate analyses. Significant P-values are shown in bold font. HR > 1, risk for death increased; HR < 1, risk for death reduced. Median relative expression of serum exosomal HOXD-AS1 was used as cut-off value for analysis.

Figures

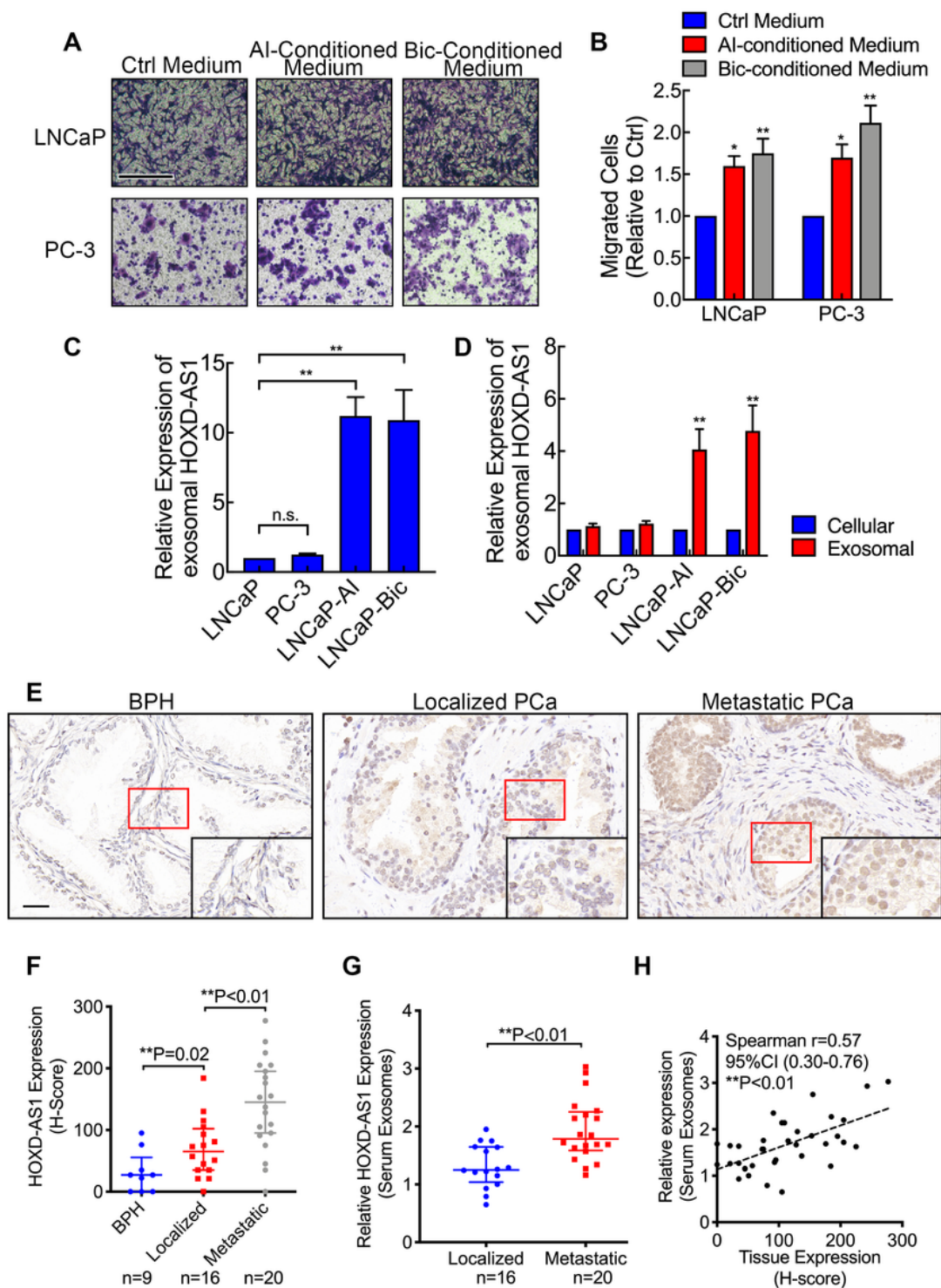


Figure 1

HOXD-AS1 is overexpressed in CRPC cell-derived and PCa patients' serum exosomes. (A-B) LNCaP and PC-3 cells were cultured with CRPC cells conditioned-medium and transwell migration assay was used to measure the migration. The results were displayed as relative ratio to control, presented as the means \pm SD of values obtained in three independent experiments. Scale bar: 200 μ m. (C) LNCaP, PC-3, LNCaP-AI and LNCaP-Bic cells were cultured for 48h and exosomes from cultural medium was collected, the

exosomal HOXD-AS1 expression was detected by qPCR. The results of real time qPCR were normalized to GAPDH and presented as the means \pm SD of values obtained in three independent experiments. (D) Cellular and exosomal HOXD-AS1 expression was compared in different PCa cells, as detected by qPCR. The results of real time qPCR were normalized to GAPDH and presented as the means \pm SD of values obtained in three independent experiments. (E) Representative images of RNA in situ hybridization (RNA-ISH) of HOXD-AS1 expression (brown) in paraffin-embedded BPH (n=9) and PCa (n=36, 16 localized and 20 metastatic) tissue. Scale bars: 50 μ m. (F) ISH of HOXD-AS1 expression was quantified by the expression score (0-300). The whiskers indicate median \pm interquartile in the plots. (G) Serum exosome was enriched from PCa patients (n=36, 16 localized and 20 metastatic) and exosomal HOXD-AS1 was detected by PCR. The results of real time qPCR were normalized to GAPDH and displayed as median \pm interquartile. (H) Correlation of HOXD-AS1 expression between PCa tissue and serum exosomes was analyzed by Spearman correlation. *p < 0.05, **p < 0.01.

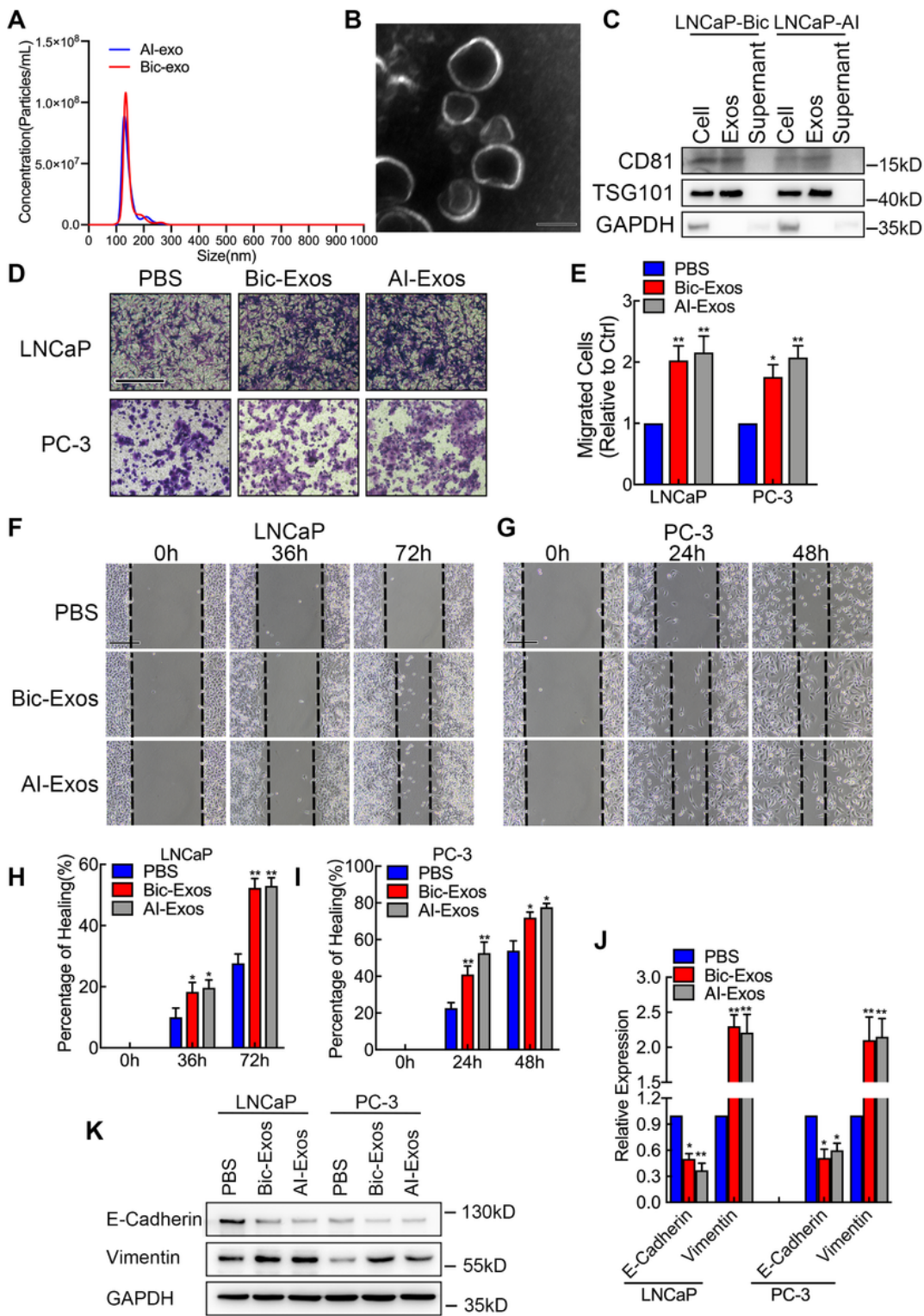


Figure 2

CRPC cell derived exosomes promotes PCa cell migration in vitro by inducing metastasis associated phenotype. (A) Purified exosomes from LNCaP-AI and LNCaP-Bic cells were analyzed by NanoSight. (B) Representative image of CRPC-exos under TEM, scale bar: 100nm. (C) Western Blot analysis of exosome markers CD81 and TSG101 in CRPC cell lysate, CRPC-exos and supernatant. (D-E) LNCaP and PC-3 cells were treated with purified CRPC-exos for 48h and the migration ability was measured by transwell

assays. The results were displayed as relative ratio to control, presented as the means \pm SD of values obtained in three independent experiments. Scale bar: 200 μ m. (F-I) LNCaP and PC-3 cells were treated with purified CRPC-exos for 48h and the cellular motility was evaluated by wound healing assay. Wound healing was measured by the percentage of healing compared with baseline and presented as means \pm SD of values obtained in three independent experiments. Scale bar: 100 μ m. (J-K) E-Cadherin and Vimentin was detected as metastatic phenotype related marker by qPCR and Western Blot. The results of real time qPCR were normalized to GAPDH and presented as the means \pm SD of values obtained in three independent experiments. *p < 0.05, **p < 0.01.

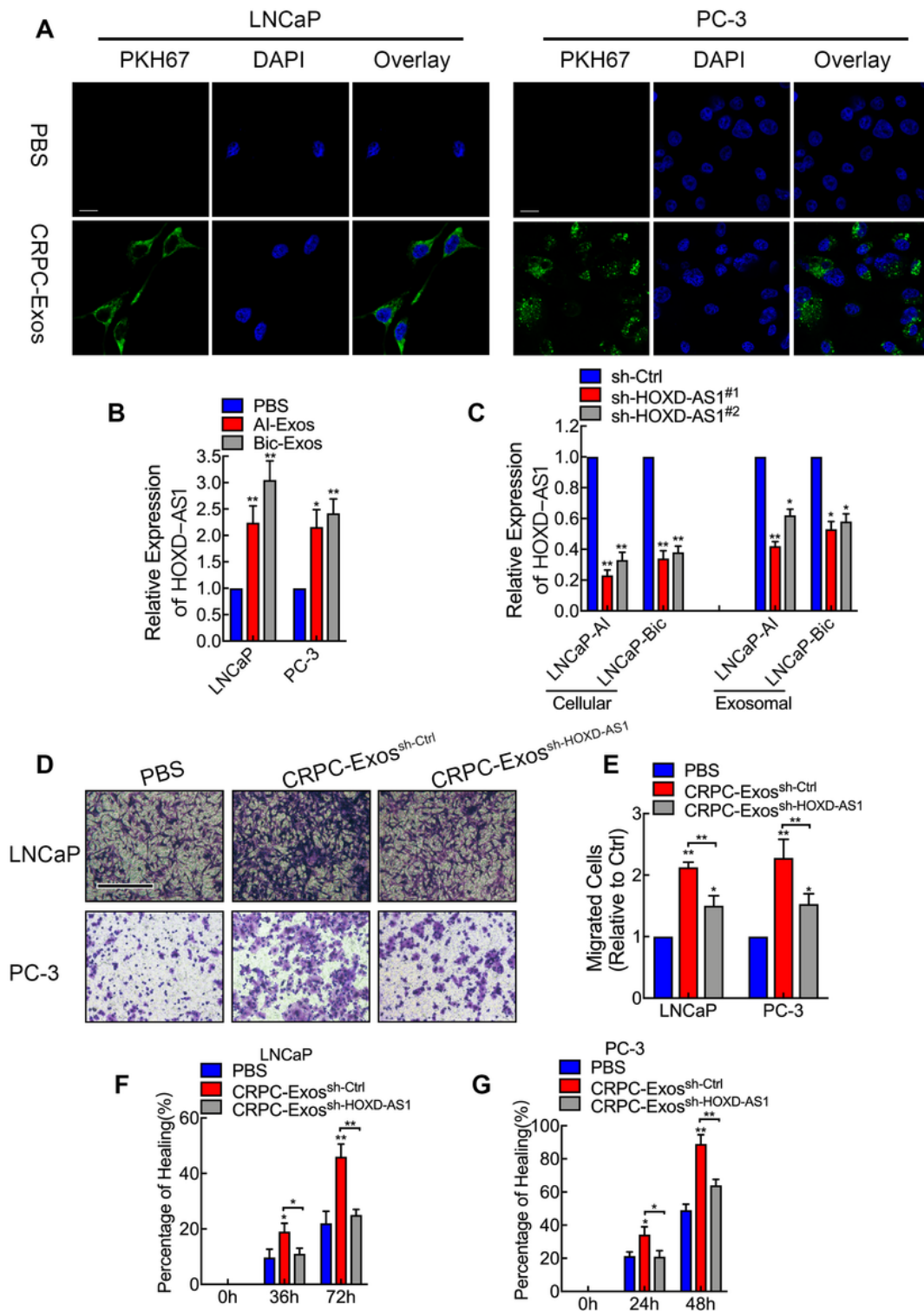


Figure 3

CRPC derived exosome enhances PCa cell motility by delivering HOXD-AS1. (A) CRPC cell secreted exosomes were labeled with PKH67(green) and incubated with PCa cells for 24h, images were captured by a confocal microscope, equal amount of PBS was used as negative control. Scale bar: 10 μ m. (B) LNCaP and PC-3 cells were incubated with purified CRPC-exos for 48h and cellular expression of HOXD-AS1 was detected by qPCR. The results of real time qPCR were normalized to GAPDH and presented as

the means \pm SD of values obtained in three independent experiments. (C) Stable HOXD-AS1 knockdown LNCaP-AI and LNCaP-Bic cells were constructed by lentiviral transduction, cellular and correspondent exosomal HOXD-AS1 was detected by qPCR. The results of real time qPCR were normalized to GAPDH and presented as the means \pm SD of values obtained in three independent experiments. (D-E) LNCaP and PC-3 cells were treated with either purified HOXD-AS1 knockdown exosomes or control exosomes for 48h, and transwell assay was conducted to measure the cellular migration, PBS were used as negative control. The results were displayed as relative ratio to control, presented as the means \pm SD of values obtained in three independent experiments. Scale bar: 200 μ m. (F-G) LNCaP and PC-3 cells were treated with either purified HOXD-AS1 knockdown exosomes or control exosomes for 48h, then cellular motility was evaluated by wound healing assay, PBS were used as negative control. Wound healing was measured by the percentage of healing compared with baseline and presented as means \pm SD of values obtained in three independent experiments. Scale bar: 100 μ m. *p < 0.05, **p < 0.01. See also Figure S1.

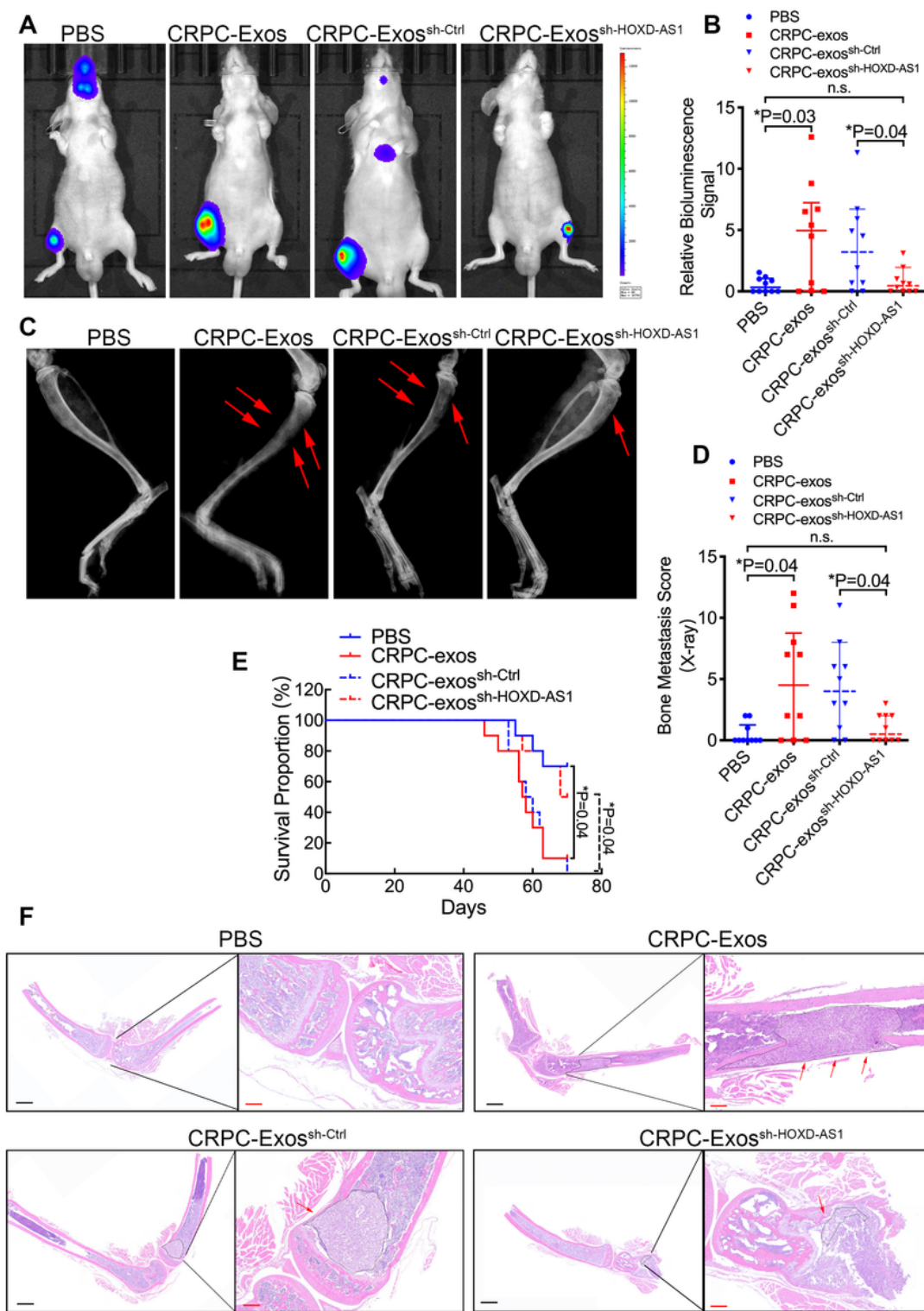


Figure 4

CRPC cell secreted exosomal HOXD-AS1 promotes distant metastasis of PCa in vivo. (A) PC-3 cells were pre-treated with either PBS or CRPC-exos, HOXD-AS1 knockdown CRPC-exos or respective control for 48h and injected intra-cardiac to mimic the process of bone metastasis. Representative bioluminescence images of bone metastasis of a mouse at 8 weeks were displayed. (B) Quantification of the bioluminescence imaging signal in the PBS and CRPC-exos groups, or HOXD-AS1 knockdown CRPC exos

and its control at 8 weeks (each n=10). (C) Representative radiographic images of bone metastasis in the indicated mice (arrows indicate osteolytic lesions). (D) The sum of bone metastasis scores for each mouse in tumor-bearing mice in each group (each n=10). (E) Kaplan-Meier analysis of bone metastasis-free survival in each group. (F) Representative images of H&E-stained sections of tibias from the indicated mouse. Arrows indicate the osteolytic lesions. Black dot-circled areas indicate the metastatic tumor in the bone. Black scale bars: 2000 μ m, red scale bars: 500 μ m. *p < 0.05, **p < 0.01.

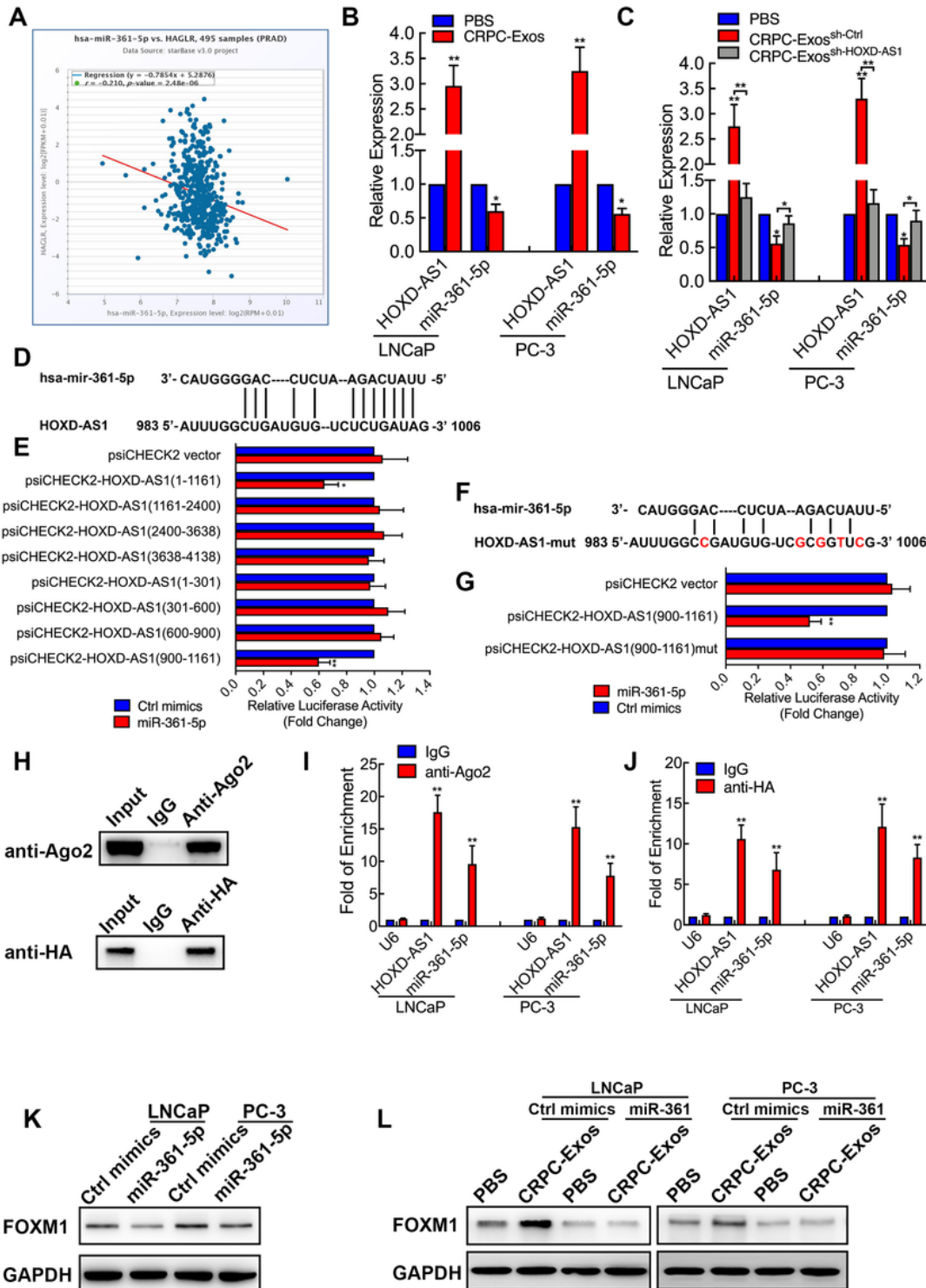


Figure 5

Exosomal HOXD-AS1 promotes PCa metastasis via miR-361-5p/FOXM1 axis. (A) The correlation of HOXD-AS1 and miR-361-5p expression in TCGA PRAD cohort was analyzed by starBase. (B) LNCaP and PC-3 cells were incubated with purified CRPC-exos for 48h, the expression of HOXD-AS1 and miR-361-5p was detected by qPCR. The results are presented as the means \pm SD of values obtained in three independent experiments. (C) LNCaP and PC-3 cells were treated with HOXD-AS1 knockdown CRPC-exos or control exosomes for 48h, the expression of HOXD-AS1 and miR-361-5p was detected by qPCR. The results are presented as the means \pm SD of values obtained in three independent experiments. (D) An illustration of the binding site between HOXD-AS1 with miR-361-5p, predicted by miRanda and starBase. (E) Different truncated HOXD-AS1 fragment was cloned into psiCHECK2 vector, and luciferase reporter assay was conducted. Empty psiCHECK2 vector was used as negative control. (F) A schematic illustration of site-directed mutagenesis on the HOXD-AS1 and miR-361-5p binding site. (G) Luciferase reporter assay was conducted using wild type or mutated HOXD-AS1 and miR-361-5p binding site. Empty psiCHECK2 vector was used as negative control. (H-J). RNA immunoprecipitation using either anti-Ago2 or anti-HA was conducted, the enrichment of Ago2 or HA was detected by Western Blot. The expression of HOXD-AS1 and miR-361-5p from the product was detected by qPCR. RNA enrichment was determined relative to the non-immuned IgG control. U6 was used as a non-specific control. The results are presented as the means \pm SD of values obtained in three independent experiments. (K) LNCaP and PC-3 cells were transfected with miR-361-5p mimics or control mimics for 48h, and FOXM1 was detected by Western Blot, GAPDH was used as an internal control. (L) LNCaP and PC-3 cells were pre-treated with CRPC-exos for 48h, then transfected with either miR-361-5p mimics or control mimics. FOXM1 expression was evaluated by Western Blot, GAPDH was used as an internal control. * $p < 0.05$, ** $p < 0.01$. See also Figure S2.

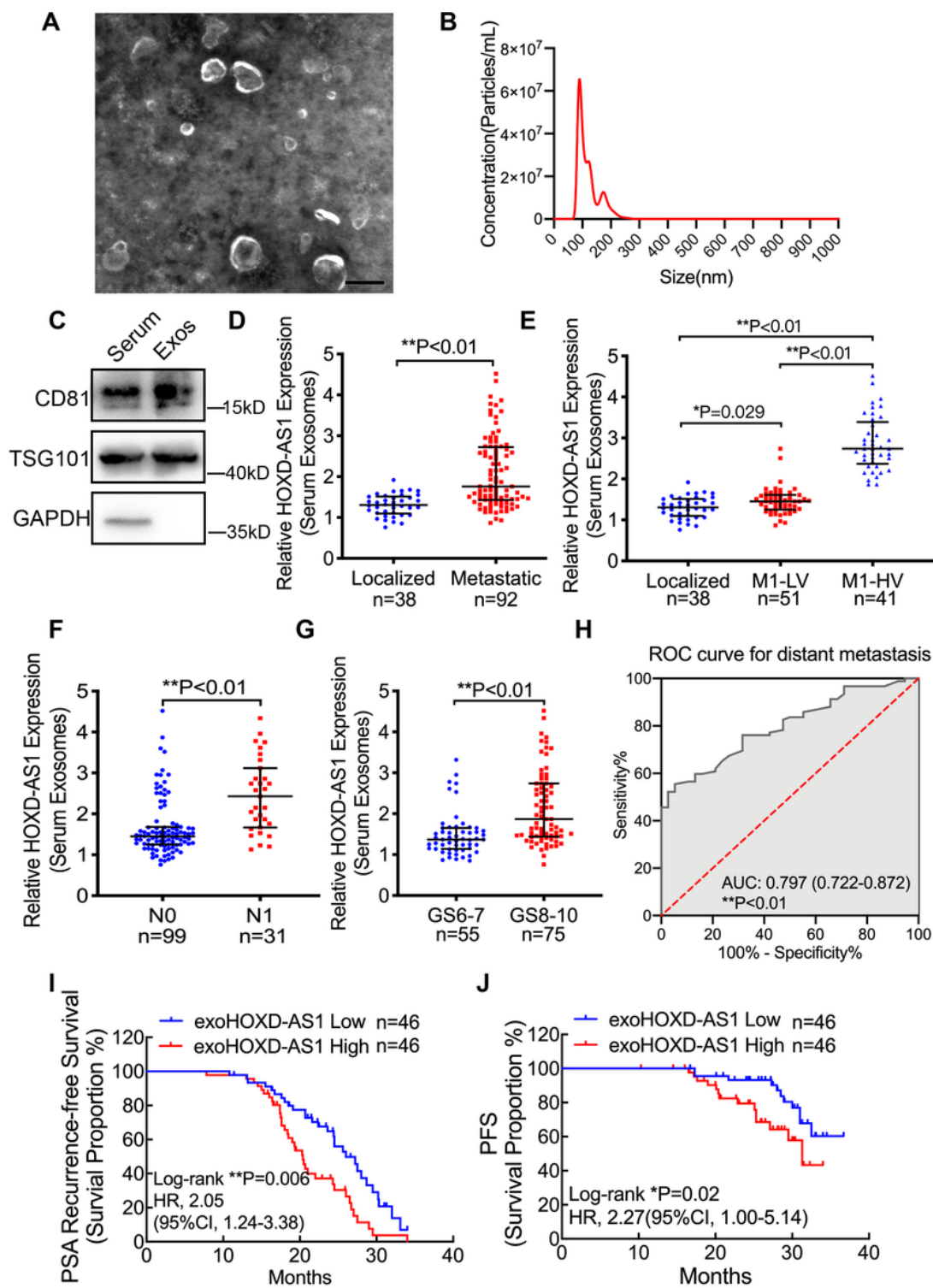


Figure 6

Serum exosomal HOXD-AS1 expression associates with clinical characteristics and prognosis in PCa. (A) Representative image of serum exosomes from PCa patients under TEM, scale bar: 100nm. (B) Purified serum exosomes from PCa patients were analyzed by NanoSight. (C) Western Blot analysis of exosome markers CD81 and TSG101 in PCa patients' serum and serum exosomes. (D) The serum exosomal HOXD-AS1 expression from PCa patients was detected by qPCR (Total n=130, localized n=38, metastatic

n=92). HOXD-AS1 expression was normalized to GAPDH, and displayed as relative expression, the whiskers indicate median and interquartile. (E) The relative expression of serum exosomal HOXD-AS1 in localized, low-volume metastatic and high-volume metastatic (indicated as M1-LV and M1-HV, respectively) PCa patients (n=38, 51, 41, respectively). The whiskers indicate median and interquartile. (F) The relative expression of serum exosomal HOXD-AS1 between non-lymph node metastasis (N0) and lymph node positive (N1) PCa patients (n=99 and 31). The whiskers indicate median and interquartile. (G) The relative expression of serum exosomal HOXD-AS1 between Gleason Score 6-7 and Gleason Score 8-10 PCa patients (n=55 and 75). The whiskers indicate median and interquartile. (H) ROC curve analysis for evaluating the diagnostic potential of serum exosomal HOXD-AS1 for distant metastasis. (I-J) The PSA recurrence-free survival and progression-free survival rates of the metastatic PCa patients were compared by Kaplan-Meier analysis in the serum exosomal HOXD-AS1-low and high groups. Median expression was used as cut off value in the survival analysis (n=92). *p < 0.05, **p < 0.01. See also Figure S3.

Supplementary Files

This is a list of supplementary files associated with this preprint. Click to download.

- [Additionalfile1TableS1.docx](#)
- [Additionalfile2TableS2.docx](#)
- [Additionalfile3TableS3.docx](#)
- [Additionalfile4SFigure1.tif](#)
- [Additionalfile5Sfigure2.tif](#)
- [Additionalfile6T12vsT34.tiff](#)
- [Additionalfile7TableS4.docx](#)
- [illustration.tif](#)